High-resolution photoabsorption cross-section measurements of SO$_2$ at 198 K from 213 to 325 nm

D. Blackie,[1] R. Blackwell-Whitehead,[2] G. Stark,[3] J. C. Pickering,[1] P. L. Smith,[4] J. Rufus,[1] and A. P. Thorne[1]

[1] SO$_2$ plays an important role in the atmospheric chemistry of the Earth, Venus, and Io. This paper presents photoabsorption cross sections of SO$_2$ from 213 to 325 nm at 198 K, encompassing the $\tilde{C}^1B_2 - \tilde{X}^1A_1$ and $\tilde{B}^1B_1 - \tilde{X}^1A_1$ electronic bands. These measurements are part of a series of measurements over the 160 to 300 K temperature range between 190 and 325 nm. The cross sections have been measured at high resolution ($\lambda/\Delta\lambda \approx 450,000$) using Fourier transform spectrometry and are compared to other high-resolution measurements in the literature.

1. Introduction

[2] This paper completes a series of reports on measurements of high-resolution UV photoabsorption cross sections of SO$_2$ at temperatures relevant to extraterrestrial atmospheres performed at Imperial College London. The measurement of SO$_2$ cross sections at 198 K in the 213 to 325 nm wavelength range is described, and the results are compared to broad band measurements in the literature, especially high-resolution measurements performed at 295 K [*Stark et al.*, 1999; *Rufus et al.*, 2003], 160 K [*Rufus et al.*, 2009] and 213 K [*Freeman et al.*, 1984] in addition to the low-resolution 200 K work of *Wu et al.* [2000].

[3] SO$_2$ is a constituent of the current terrestrial atmosphere, the atmosphere of the early Earth, and the atmospheres of Venus and Io. SO$_2$ is one of the most important and well studied molecules in the atmosphere of Venus [e.g., *Pollack et al.*, 1980; *Na et al.*, 1990, 1994; *Bertaux et al.*, 1996; *Mills and Allen*, 2007; *Bertaux et al.*, 2007]. SO$_2$ has been detected in the UV spectrum of light scattered by the upper cloud layers and is observed in the Venusian atmosphere down to the surface level. The SO$_2$ features detected at the upper limits of the cloud layers represent the highest altitude at which SO$_2$ appears in the Venusian atmosphere due to rapid photodissociation of the molecule by solar UV radiation above the cloud layers [*de Bergh et al.*, 2006]. The photodissociation of SO$_2$ drives the Venusian sulfur cycle, and so affects the cloud chemistry. At the surface level, it has been suggested [*Hashimoto and Abe*, 2005] that SO$_2$ is involved in interactions with carbonates or pyrites. Interactions between SO$_2$ and the Venusian surface would affect the amount of SO$_2$ required to be injected directly by volcanic activity into the atmosphere to maintain the composition of the Venusian atmosphere, thereby informing models of the internal dynamics of the planet [*Taylor and Grinspoon*, 2009]. The measurement of the vertical distribution of SO$_2$ at UV wavelengths, and the measurement of the concentration of SO$_2$ at the cloud tops, are prime objectives of SPICAV and other instruments on board the Venus Express mission [*Bertaux et al.*, 2007; *Svedhem et al.*, 2007].

[4] SO$_2$ is also prominent in the atmosphere of the volcanically active Jovian moon Io [*Ballester et al.*, 1994; *Sartoretti et al.*, 1996; *Hendrix et al.*, 1999; *Lellouch*, 2005]. The New Horizons flyby is the latest mission to study Io, detecting ten SO$_2$-rich "Prometheus style" plumes [*Spencer et al.*, 2007]. Uncertainty still remains about the relative contributions of volcanic plumes and surface frost sublimation as mechanisms for the deposition of SO$_2$ into Io's atmosphere.

[5] The accurate chemical abundance analysis of both the Venusian and Ionian atmospheres has been limited by the lack of laboratory photoabsorption cross sections measured at high resolution at temperatures relevant to planetary atmospheres. Low-resolution laboratory absorption measurements disguise the effects of saturation and lead to systematic underestimates of the cross sections of narrow spectral features.

[6] The measurement of photoabsorption cross sections at a resolution sufficient to resolve the line profiles, and at a

[1]Space and Atmospheric Physics Group, Imperial College London, London, UK.
[2]Lund Observatory, Lund, Sweden.
[3]Department of Physics, Wellesley College, Wellesley, Massachusetts, USA.
[4]Harvard-Smithsonian Center for Astrophysics, Cambridge, Massachusetts, USA.

Table 1. The Resolving Power, Wavelength Range, and Temperature of SO$_2$ Photoabsorption Cross-Section Measurements in the Literature

Reference	Resolving Power	Spectral Range (nm)	Temperature (K)
Present work	≈450,000	220–325	198
Hermans et al. [2009]	13,250	227–345	345–420
Rufus et al. [2009]	≈420,000	190–220	160
Danielache et al. [2008]	2,000	190–330	293
Rufus et al. [2003]	≈450,000	220–325	295
Bogumil et al. [2003]	1,040	239–395	203–293
Wu et al. [2000]	5,200	208–295	400, 295, 200
Stark et al. [1999]	450,000	198–220	295
Koplow et al. [1998]	1.5×10^8	215.21–215.23	295
Vattulainen et al. [1997]	600	200–400	295–800
Prahlad et al. [1996]	3,000	280–320	220–300
Vandaele et al. [1994]	16,600	250–370	295
Manatt and Lane [1993]	2,500	106–403	295
Ahmed and Kumar [1992]	1,250	188–231	295
Ahmed and Kumar [1992]	1,250	279–320	295
Martinez and Joens [1992]	2,200	197–240	295
Hearn and Joens [1991]	4,725	228–339	300
McGee and Burris [1987]	10,400	300–324	295, 210
Freeman et al. [1984]	200,000	172–240	213
Brassington et al. [1984]	600,000	299.2–300.12	295
Wu and Judge [1981]	4,560	208–228	295
Wu and Judge [1981]	4,560	299–340	295
Brassington [1981]	6,000	290–317	295
Marx et al. [1980]	1.5×10^6	299.917–300.14	295
Woods et al. [1984]	1.5×10^5	297–301	295

range of temperatures comparable to those of planetary atmospheres, is necessary to account for the temperature dependence of the UV photoabsorption cross sections of SO$_2$. A complete spectroscopic analysis of the SO$_2$ spectrum has not been made, so that it is not possible to calculate reliably, from room temperature measurements, the cross sections at the lower temperatures of Io (150 to 250 K [*Jessup et al.*, 2004]) and the cloud layers of Venus (180 to 230 K [*Zasova et al.*, 2007]). Direct measurements of the cross sections at comparably low temperatures are therefore important for improving the atmospheric modeling.

[7] Sulfur dioxide is also a key component of the Earth's sulfur cycle. SO$_2$ is directly injected into the atmosphere through volcanic activity and industrial processes. In addition, SO$_2$ is produced through in situ atmospheric reactions involving H$_2$S and dimethyl sulphide. SO$_2$ is regarded as an important terrestrial atmospheric gas due to its ability to form H$_2$SO$_4$, which can then precipitate into oceans and groundwater supplies [*Swedish Environmental Protection Agency*, 1990; *Speidel et al.*, 2007; *Krotkov et al.*, 2008]. Furthermore, the study of the early Earth's sulfur cycle could allow greater understanding of the composition and evolution of the atmosphere of the early Earth. The timing of the oxygenation of the Earth's atmosphere is a central issue in the understanding of the Earth's paleoclimate. The discovery of mass-independent fractionation (MIF) of sulfur isotopes deposited within Archean and Paleoproterozoic rock samples has given rise to a possible marker, through the transition between MIF within older rock samples (>2.4 Gyr) to mass-dependent fractionation found in younger rock samples, for the rise in oxygen concentrations within the Earth's atmosphere [*Farquhar et al.*, 2000, 2001; *Farquhar*

and Wing, 2003]. The introduction of high-resolution cross sections into these atmospheric models will allow a more accurate interpretation of the sulfur isotope ratios found in ancient rock samples [*Lyons*, 2007]. An ongoing extension to the cross-section measurements that are presented here is the measurement of the individual sulfur isotopologues of SO$_2$ at UV wavelengths.

1.1. The UV SO$_2$ Spectrum

[8] The complex structure of the UV SO$_2$ spectrum has been the subject of multiple experimental and theoretical investigations. The spectrum of the SO$_2$ molecule in the 213 to 325 nm spectral range is dominated by two absorption systems separated by a region of comparatively low cross section. The most prominent absorption system extends from 170 to 230 nm and is associated with the transition from the ground $\tilde{X}^1A_1$ state to the excited $\tilde{C}^1B_2$ electronic state. The second absorption system is weaker, extending from 240 to 340 nm, and is attributed to the $\tilde{B}^1B_1 - \tilde{X}^1A_1$ transition. However, previous work [*Kullmer*, 1985] demonstrated the hybrid nature of the $\tilde{B}^1B_1 - \tilde{X}^1A_1$ transition, citing additional contributions from the $^3B_1$, $^3B_2$, and $^1A_2$ states. Both the $\tilde{C}^1B_2 - \tilde{X}^1A_1$ and the $\tilde{B}^1B_1 - \tilde{X}^1A_1$ systems show long progressions in v'_1 and v'_2 as expected from the Franck-Condon principle [*Herzberg*, 1966].

1.2. Previous Laboratory Measurements of the SO$_2$ Spectrum

[9] The first laboratory measurements of SO$_2$ [*Clements*, 1935] provided the basis for the research of *Shaw et al.* [1980], who first assigned the vibronic bands of the $^1B_1$ state. This led to the development of a simplified model of

Table 2. Experimental Details: Wavelength Range, Gas Sample Pressure, Resolution, and PMT Detector Used[a]

Wavelength Range (nm)	Pressure (Torr)	Resolution (cm^{-1})	PMT
308.4–325.0	9.4, 6.6	0.06	1P28
294.8–308.4	9.4, 1.5	0.06	1P28
282.9–294.8	3.8, 2.2	0.06	1P28
282.9–294.8	4.0, 2.0	0.09	R166
263.5–282.9	3.9, 2.1	0.09	R166
246.9–263.5	9.4, 7.8	0.09	R166
233.6–246.9	9.5, 9.9	0.50	R166
220.0–233.6	9.6, 4.9	0.30	R166
220.0–226.7	2.0, 2.8	0.30	R166
215.9–220.0	0.130, 0.203	0.12	R166
212.6–215.9	0.159, 0.084	0.12	R166

[a]The actual band passes of the monochromator extend about ±2 nm beyond the ranges quoted here to allow the overlap of adjacent wavelength sections.

the multilevel vibronic coupling [*Kullmer*, 1985]. Experiments using laser induced fluorescence (LIF) have studied the vibrational bands of SO$_2$ with resolutions as high as 0.08 cm^{-1} but over a limited wavelength range [e.g., *Shaw et al.*, 1980; *Ebata et al.*, 1988; *Yamanouchi*, 1995; *Katagiri et al.*, 1997; *Hegazi et al.*, 1998; *Sako et al.*, 1998]. Vibrational assignments have been made for the majority of the bands up to the dissociation limit.

[10] LIF has been used by a series of authors to define the predissociation limit of the SO$_2$ molecule at 218.7 nm [e.g., *Katagiri et al.*, 1997]. While line broadening is expected below this limit, *Katagiri et al.* [1997] reported insignificant broadening down to 210 nm.

[11] Table 1 summarizes the wavelength range, resolution, and temperature of cross-section measurements in the literature to date. It can be seen from Table 1 that the only measurements of comparable resolution and wavelength range to the absorption cross sections presented in this paper are the previous measurements in this series of *Stark et al.* [1999] and *Rufus et al.* [2003, 2009]. Measurements performed by *Freeman et al.* [1984] were carried out with a resolving power of approximately half that used in the present measurements. The remainder of the broad-

band cross-section measurements were made at resolving powers at least an order of magnitude less than those reported here.

[12] The LIF measurements of *Koplow et al.* [1998] have resolving powers 3 orders of magnitude greater than the measurements presented in this paper, but only over an extremely limited spectral range (215.21 to 215.23 nm).

2. Experimental Procedure

[13] The SO$_2$ photoabsorption cross-section measurements were made with the Imperial College ultraviolet Fourier transform spectrometer (IC UV FTS) [*Thorne et al.*, 1987] with a 300 W Hamamatsu xenon arc lamp as a continuum light source. The IC UV FTS has a maximum resolution of 0.025 cm^{-1}, which is sufficient to fully resolve the Doppler width of SO$_2$ lines at 198 K, 0.057 cm^{-1} ($\approx$0.00028 nm) at 220 nm. The measured widths of absorption features are expected to be larger than the calculated Doppler width due to blending of lines resulting from the high number of bands and lines observed within the $\tilde{C} - \tilde{X}$ electronic system. The resolution of the measurements was constrained by experimental factors, such as the requirement to achieve a satisfactory signal-to-noise ratio (SNR), and the ability to keep gas pressures and temperatures stable for the duration of the experiment, up to 18 h. A range of resolution from 0.06 cm^{-1} for the highly structured band features, to 0.5 cm^{-1} for the continuum region between the electronic bands was used, matching that of the previous measurements performed at Imperial College at 295 K and 160 K [*Stark et al.*, 1999; *Rufus et al.* 2003, 2009].

[14] The input to the FTS was band limited with a zero-dispersion monochromator [*Murray*, 1992] in order to improve SNR in the spectrum and to allow optimum photomultiplier tube detectors (PMTs) and gas column densities to be chosen for each spectral band. Two types of Hamamatsu PMTs were used: (1) R166 for the 212 to 295 nm region and (2) 1P28 for the 282 to 325 nm region. The SO$_2$ gas, in natural abundance, was supplied by BOC with a purity of 99.9%. Two capacitance manometer pressure gauges recorded
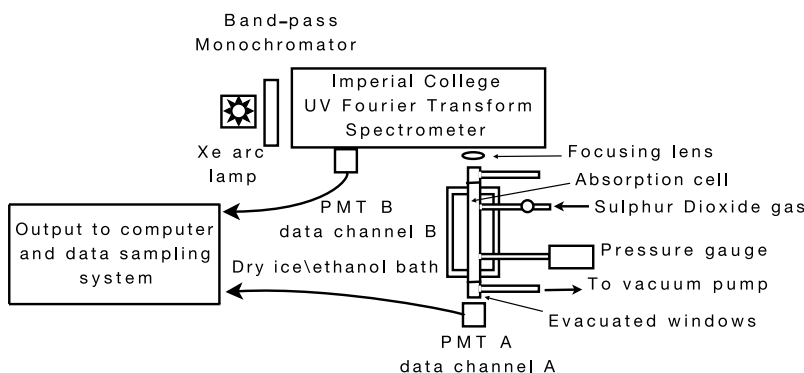

Figure 1. The positioning of the absorption cell in the second output when using the "dual output" technique for absorption spectroscopy.

Table 3. The Contributing Uncertainties and Final Error Budget for Our Measurements of the Photoabsorption Cross Sections of SO$_2$

	Uncertainty (%)	
	$\sigma \approx 1 \times 10^{-17}$ cm^2	$\sigma \approx 1 \times 10^{-18}$ cm^2
Column density (N) total	2.9%	2.5%
Contributing errors for (N)		
Temperature	0.5%	0.5%
Column length	0.25%	0.25%
Pressure reading	2.8%	2.1%
SNR	7%	14%
I/I_0	4.5%	4.5%
Percentage uncertainty	8.8%	14.9%

the pressure in the absorption cell, a 10 Torr MKS 122AA and a 1 Torr MKS 220CA.

[15] The 213 to 325 nm wavelength range of this study was divided into 10 sections, each with a 2 to 3 nm overlap with the adjacent sections. Measurements of the individual sections were combined into a spectrum covering the full 213 to 325 nm range. Each wavelength section was recorded at two different gas pressures to enable the optical depth of the absorption spectrum to be examined for signs of saturation. Agreement between the peak cross-section values of the high- and low-pressure measurements was within 5% for each spectral region. Where possible the cross sections recorded from the lower-pressure measurements were used in the final tabulation. The cross sections were convolved down to a matching resolution to allow an accurate comparison of the cross sections in adjacent wavelength regions, before being linked together. The cross sections within the overlap of adjacent wavelength regions agreed on average to within 2%. Table 2 shows the resolution, detector, and gas pressures used to record each wavelength section.

[16] The coolable absorption cell had a path length of 9.4 cm. The main outer cell body was constructed of stainless steel and submerged in a coolant bath of dry ice and ethanol. This mixture maintained the absorption cell at 198 K, with the temperature being monitored by a low-temperature alcohol thermometer. At both ends of the cell a double-layer silica window, consisting of two silica windows separated by a 3 cm evacuated region, prevented water condensation from the ambient laboratory air.

[17] The absorption cross section is calculated from the Beer-Lambert law,

$$\sigma(\lambda) = \frac{1}{N} \ln\left[\frac{I_0(\lambda)}{I(\lambda)}\right] \qquad (1)$$

where $I_0(\lambda)$ is the incident intensity, $I(\lambda)$ is the transmitted intensity through the gas column, and N is the column density. We used the second output beam of the IC UV FTS to address possible problems with long- and short-term fluctuations of the Xe lamp output [Pebler and Zomp, 1981]. As shown in Figure 1, the absorption cell was placed in one of the two FTS output beams with a PMT to record $I(\lambda)$, while a second PMT at the second output simultaneously recorded $I_0(\lambda)$. Low-resolution "before" and "after" scans with the cell evacuated established the ratio of the intensities and the PMT

responses at the two outputs, and the ratio of the two outputs then gave $I_0(\lambda)/I(\lambda)$, with drifts and fluctuations ratioed out. The target SNR of 70 to 100, measured near the continuum level in regions of low absorption, was achieved by coadding up to 256 interferograms, each of approximately 85 s, giving a total integration time for each spectral region of approximately 6 h.

[18] FTS uses the fringe intervals of a reference HeNe laser to generate an accurately linear wavenumber scale, with the accuracy of the scale being limited by the stability of the laser which is 1 part in 10^8. This is put on an absolute scale by measurement of reference spectral lines of known wavenumber. In principle only a single line is required, but in practice several lines are used to reduce the uncertainty.

[19] The IC UV FTS wavenumber scale was calibrated through measurement of the spectrum of an iron hollow cathode lamp run at a current of 15 mA. Measured Fe spectral lines were compared to accurately known wavenumbers for Fe I and Fe II lines [Nave et al., 1991] giving a calibration factor α in the equation: $\overline{\sigma}_{obs} = \overline{\sigma}_{true}(1 - \alpha)$. The wavenumber uncertainly associated with this single measurement is $\approx$0.0025 cm^{-1}, however, the calibration factor varies with slight changes in the spectrometer optical alignment from day to day. In previous measurements [Blackwell-Whitehead, 2003], day to day variations in the value of the calibration factor of up to 55% were measured. Since the iron calibration spectrum was recorded some time after the SO$_2$ spectral measurements, taking the possible typical variation in instrument calibration factor into account, the uncertainly of the combined wavenumber scale is 0.04 cm^{-1}.

[20] Stark et al. [1999] derived an expression for the fractional uncertainty in the measured SO$_2$ cross section at any wavelength:

$$\frac{\Delta\sigma}{\sigma} = \left[\left(\frac{\Delta N}{N}\right)^2 + \left(\frac{1}{(\mathrm{SNR})N\sigma}\right)^2 \left\{1 + e^{2N\sigma}\right\}\right]^{1/2} \qquad (2)$$

Within the square root, the first term represents the fractional uncertainty in the column density (N) incorporating uncertainties in the gas temperature and pressure and path length through the gas sample, and the second term represents the uncertainty due to the SNR and the depth of absorption. The estimated uncertainty in the column density, dependent upon the gas pressure and temperature in the absorption cell, ranged between 2.1 and 2.8%.

[21] An additional source of uncertainty stems from a decrease in the transmission efficiency of the internal cell windows due to adsorption of SO$_2$, despite the fact that the cell pressure was well below the saturated vapor pressure. Such adsorption has been documented by Prahlad et al. [1996] with carbon tetrachloride and by Wu et al. [1989] with acetylene. Tests were conducted on the absorption cell to determine the reduction of transmission of the internal silica windows due to the adsorption of SO$_2$, with the maximum observed decrease in the light intensity ($I_0(\lambda)$) passing through the cell being 5.5%.

[22] With the dual output method allowing simultaneous measurement of $I(\lambda)$ and $I_0(\lambda)$, the stability of the relative sensitivities of the two PMTs is vital for obtaining an
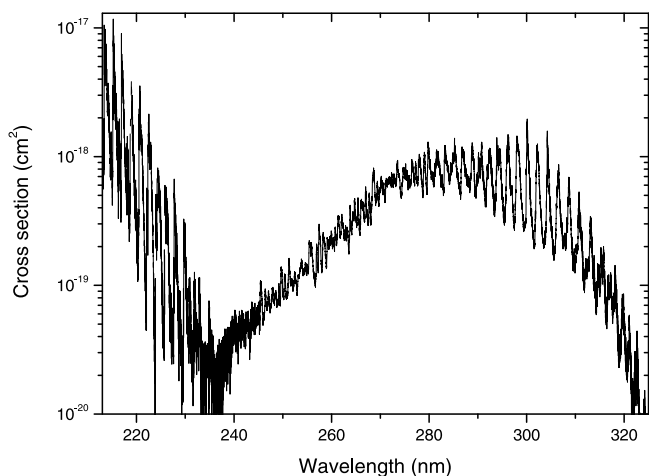
Figure 2. Photoabsorption cross sections for SO_2 in the 213 to 325 nm wavelength region at 198 K, smoothed using a 0.008 nm filter.

accurate $I(\lambda)/I_0(\lambda)$ ratio. In order to minimize the drift in the relative sensitivities of the two PMTs, several precautions were used. First, the two PMTs were selected from the same manufactured batch in order to minimize differences in construction or dopant materials; second, the two PMTs were only used as a pair so as to maintain a common light-exposure history; and finally they were operated in a temperature-stabilized environment. Laboratory tests, each over a 7 h period, indicated a wavelength independent 2.2% average relative drift in sensitivity between the two PMTs.

[23] However, the effect of PMT drift and the adsorption of SO_2 by the cell windows will be observable in the change in value for the low-resolution evacuated cell scans before and after the main gas measurements. The average difference between the before and after values was 1.8%. This uncertainty when considered on an absorption feature with an absorption depth of 60% gives an uncertainty of 4.5% in the value of I/I_0.

[24] The uncertainties for the measurements of the photoabsorption cross sections of SO_2 is shown in Table 3. The total estimated fractional uncertainty in our derived cross sections, determined by combining the contributions described above, is dependent upon the strength of the photoabsorption cross sections and ranges from ±8.8% in regions of high cross section ($\sigma \approx 1 \times 10^{-17}$ cm^2) to ±14.9% in regions of low cross section ($\sigma \approx 1 \times 10^{-18}$ cm^2).

3. Results

[25] Figure 2 shows the measured cross sections of SO_2 at 198 K, smoothed for clarity of presentation using an 0.008 nm filter, across the 213 to 325 nm range. A full tabulation of the cross sections can be found in the appendix (numerical tabulations of the cross sections presented in this paper, in addition to those from *Stark et al.* [1999] and *Rufus et al.* [2003, 2009] can be found at ftp://ftp.agu.org/apend/je/2010JE003707/).
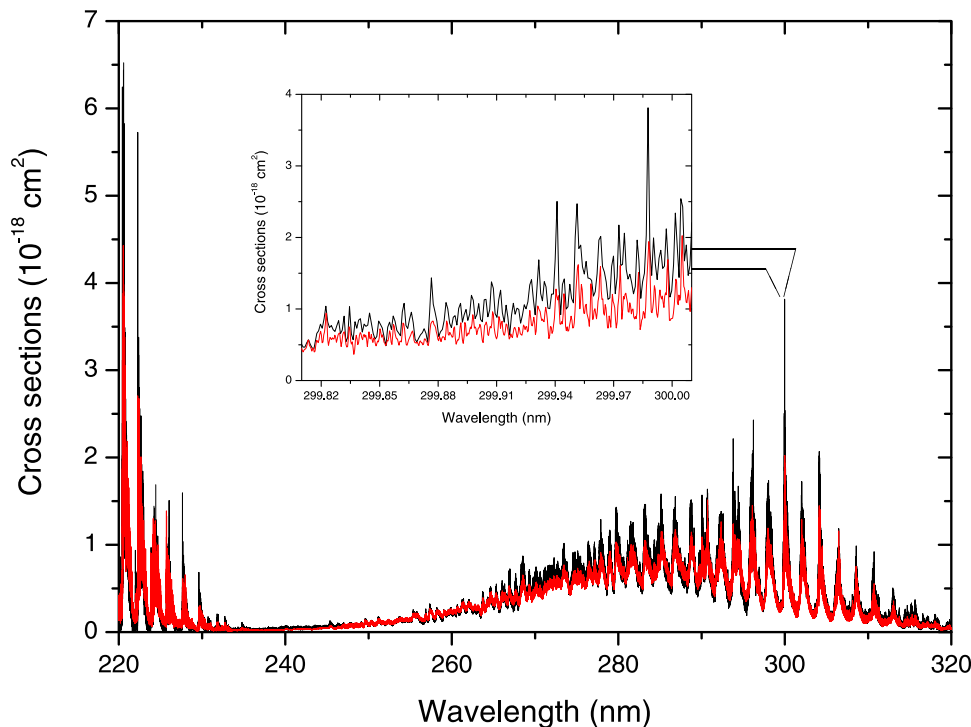

Figure 3. The measured high-resolution photoabsorption cross sections of SO_2 as measured by *Rufus et al.* [2003] at 295 K (red) and the current work at 198 K (black), with structure in a 0.2 nm region shown in the inset.
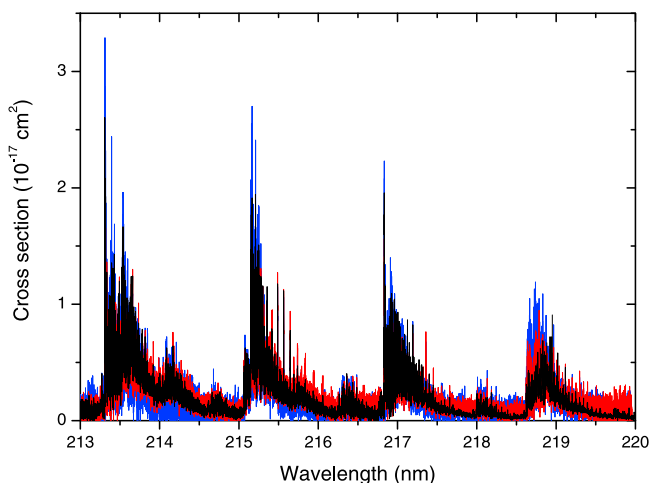
Figure 4. The three sets of high-resolution cross sections of SO_2 recorded at Imperial College in the 213 to 220 nm range, 160 K [*Rufus et al.*, 2009] (blue), 198 K current measurements (black), and 295 K [*Stark et al.*, 1999] (red).

3.1. Comparison With Other High-Resolution Data Sets Measured at Imperial College

[26] A change in temperature will result in a change in the percentage of SO_2 molecules in a particular vibrational state. At temperatures below room temperature (T < 295 K) the majority of molecules will be in the ground vibrational states. *Rufus et al.* [2009] calculated that at 295 K ≈92% of the molecules will be in the (0,0,0) state, with ≈7% being in the (0,1,0) state. At 198 K, using fundamental values for the vibrational quanta published by *Herzberg* [1966], the calculated percentage population of molecules in the (0,0,0) state should be ≈97% with ≈2.2% in the (0,1,0) state. This relatively small change in population distribution only marginally affects the photoabsorption cross section. There will however be an expected change in the shape of the spectral lines with the change in gas temperature. The spectral lines are expected to have a greater peak cross section but with a reduced line width at lower temperatures due to a decrease in the Doppler widths maintaining a constant integrated cross section at all temperatures. The predicted Doppler width increases from 0.057 cm^{-1} (≈0.00028 nm) to 0.07 cm^{-1} (≈0.00033 nm) at 220 nm as the temperature increases from 198 K to 295 K.

[27] Figure 3 shows the current 198 K absorption cross-section measurements compared with the 295 K measurements of *Rufus et al.* [2003]. These two sets of measurements were made on the IC UV FTS at comparable resolutions. It can be seen that the values of the cross sections at the band peaks are significantly higher within the $\tilde{B}^1B_1 - \tilde{X}^1A_1$ transition at 198 K than at 295 K. The integrated cross section from 235 to 325 nm at 198 K is 8% larger than that of the spectrum at 295 K; this difference is within the stated uncertainties of the two sets of measurements.

[28] Figure 4 shows the three sets of absorption cross-section measurements between 213 and 220 nm made at Imperial College on the IC UV FTS: at 295 K [*Stark et al.*, 1999], the current measurements at 198 K, and at 160 K [*Rufus et al.*, 2009]. It can be seen that the peak cross-section value for each vibrational band increases as the temperature at which the cross sections were measured decreases. Figure 5 shows an expanded section of Figure 4. This shows that the cross sections of the strongest transitions at the band head are significantly increased at lower temperatures, demonstrating the temperature dependence of the rotational population of the lower level.

3.2. Comparison With Other Data Sets

[29] Our results can be compared with previously published results. *Freeman et al.* [1984] measured the photoabsorption cross sections of SO_2 at 213 K with resolutions between 0.4 and 0.1 cm^{-1}. This resolution is high enough to successfully avoid strong saturation effects. However, even small differences in resolution between high-resolution data sets can have a significant effect when used in atmospheric modeling. *Jessup et al.* [2004] identified a 10% overestimate in the density of SO_2 within Io's atmosphere due to using the 0.41 cm^{-1} FWHM cross sections from *Freeman et al.* [1984] as compared to the 0.14 cm^{-1} FWHM cross sections of *Rufus et al.* [2009, 2003].

[30] Agreement well within the quoted experimental errors between this work and that of *Wu et al.* [2000] is observed in regions of the spectrum with broad continuum-like structure. On the other hand Figure 6 shows significant differences in the absorption cross sections between the high- and low-resolution spectra when observing the fine detail of the $\tilde{C}$ (1,5,2) − $\tilde{X}$ (0,0,0) band (vibrational assignments by *Okazaki et al.* [1997]). The differences in the recorded cross sections are most prominent in the sharp peaks of the UV SO_2 spectrum and are mainly attributed to the difference in resolution between our work and that of
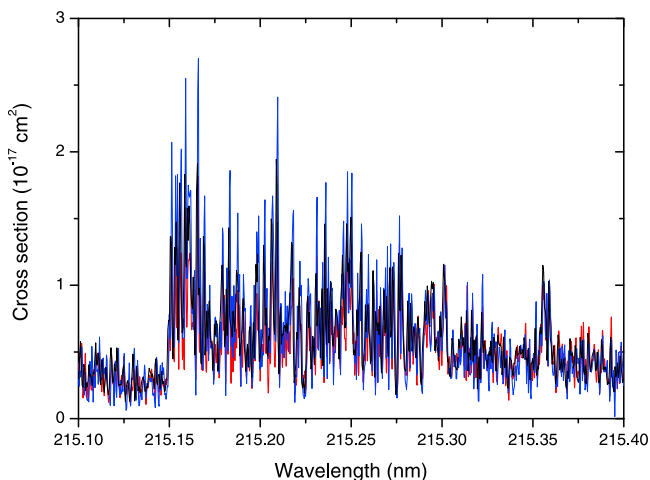

Figure 5. A single vibrational band in the three sets of high-resolution cross sections of SO_2 measured at Imperial College, 160 K [*Rufus et al.*, 2009] (blue), 198 K current measurements (black), and 295 K [*Stark et al.*, 1999] (red).
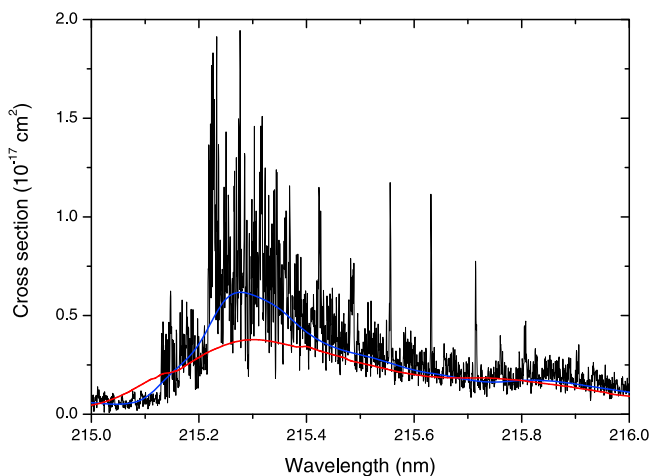
Figure 6. Measured high resolution (black) ($\Delta\lambda = 0.00056$ nm), low resolution (red) ($\Delta\lambda = 0.05$ nm by *Wu et al.* [2000]), and measured high resolution convolved with a Gaussian profile of 0.05 nm FWHM (blue) SO₂ photoabsorption cross sections of the $\tilde{C}$ (1,5,2) $- \tilde{X}$ (0,0,0) (vibrational assignments by *Okazaki et al.* [1997]).

Wu et al. [2000]. Figure 6 also shows the measurements presented in this paper convolved with a Gaussian profile of 0.05 nm (FWHM) in order to remove the effect of resolution between the two measurements. However, significant differences in the measured cross sections at shorter wavelengths are still observed between the two measurements with the convolved high-resolution data having band peaks of approximately 1/3 greater than those recorded by *Wu et al.* [2000]. The difference between the two data sets, even when compared at identical resolution, can be attributed to undetected saturation of the strong absorption lines during lower-resolution measurements.

4. Conclusion

[31] High-resolution UV photoabsorption cross sections of SO₂ have been measured between 213 and 325 nm at 198 K. These measurements represent the final part of a campaign at Imperial College to measure the photoabsorption cross sections of SO₂ at wavelengths and temperatures relevant to planetary atmospheres. The 198 K measurements complement the room temperature measurements of *Rufus et al.* [2003] over the same wavelength region and at identical resolution. The two data sets significantly increase the resolution (resolving power ≈450,000) and temperature range at which cross sections are available for the analysis and modeling of planetary atmospheres. Numerical wavenumber tabulations of our SO₂ cross sections can be obtained from the auxiliary material, from the authors and are also available at http://cfa-www.harvard.edu/amdata/ampdata/cfamols.html.[1]

---

[1]Auxiliary materials are available at ftp://ftp.agu.org/apend/je/2010je003707.

References

Ahmed, S. M., and V. Kumar (1992), Quantitative photoabsorption and fluorescence spectroscopy of SO₂ at 188–231 and 278.7–320 nm, *J. Quant. Spectrosc. Radiat. Transfer*, *47*, 359–373, doi:10.1016/0022-4073(92)90038-6.

Ballester, G. E., M. A. McGrath, D. F. Stobel, X. Zhu, P. D. Feldman, and H. W. Moos (1994), Detection of the SO₂ atmosphere on Io with the Hubble Space Telescope, *Icarus*, *111*, 2–17, doi:10.1006/icar.1994.1129.

Bertaux, J.-L., T. Widemann, A. Hauchecorne, V. I. Moroz, and A. P. Ekonomov (1996), VEGA 1 and VEGA 2 entry probes: An investigation of local UV absorption (220–400 nm) in the atmosphere of Venus (SO₂ aerosols, cloud structure), *J. Geophys. Res.*, *101*, 12,709–12,745, doi:10.1029/96JE00466.

Bertaux, J.-L., et al. (2007), SPICAV on Venus Express: Three spectrometers to study the global structure and composition of the Venus atmosphere, *Planet. Space Sci.*, *55*, 1673–1700, doi:10.1016/j.pss.2007.01.016.

Blackwell-Whitehead, R. (2003), High resolution Fourier transform spectroscopy of the spectrum of neutral manganese, Ph.D. thesis, Imperial Coll. London, London.

Bogumil, K., et al. (2003), Measurements of molecular absorption spectra with the SCIAMACHY pre-flight model: Instrument characterization and reference data for atmospheric remote-sensing in the 230–2380 nm region, in *Atmospheric Photochemistry*, edited by J. P. Burrows and G. K. Moortgat, *J. Photochem. Photobiol., A*, *157*(2–3), 167–184, doi:10.1016/S1010-6030(03)00062-5.

Brassington, D. J. (1981), Sulfur dioxide absorption cross-section measurements from 290 nm to 317 nm, *Appl. Opt.*, *20*, 3774–3779.

Brassington, D. J., R. C. Felton, B. W. Jolliffe, B. R. Marx, J. T. M. Moncrieff, W. R. C. Rowley, and P. T. Woods (1984), Errors in spectroscopic measurements of SO₂ due to nonexponential absorption of laser radiation, with application to the remote monitoring of atmospheric pollutants, *Appl. Opt.*, *23*, 469–475.

Clements, J. H. (1935), On the absorption spectrum of sulphur dioxide, *Phys. Rev.*, *47*, 224–232, doi:10.1103/PhysRev.47.224.

Danielache, S. O., C. Eskebjerg, M. S. Johnson, Y. Ueno, and N. Yoshida (2008), High-precision spectroscopy of ³²S, ³³S, and ³⁴S sulfur dioxide: Ultraviolet absorption cross sections and isotope effects, *J. Geophys. Res.*, *113*, D17314, doi:10.1029/2007JD009695.

de Bergh, C., V. I. Moroz, F. W. Taylor, D. Crisp, B. Bézard, and L. V. Zasova (2006), The composition of the atmosphere of Venus below 100 km altitude: An overview, *Planet. Space Sci.*, *54*, 1389–1397, doi:10.1016/j.pss.2006.04.020.

Ebata, T., O. Nakazawa, and M. Ito (1988), Rovibrational dependences of the predissociation in the ¹B₂ state of SO₂, *Chem. Phys. Lett.*, *143*, 31–37, doi:10.1016/0009-2614(88)87006-4.

Farquhar, J., and B. A. Wing (2003), Multiple sulfur isotopes and the evolution of the atmosphere, *Earth Planet. Sci. Lett.*, *213*, 1–13, doi:10.1016/S0012-821X(03)00296-6.

Farquhar, J., J. Savarino, T. L. Jackson, and M. H. Thiemens (2000), Evidence of atmospheric sulphur in the Martian regolith from sulphur isotopes in meteorites, *Nature*, *404*, 50–52.

Farquhar, J., J. Savarino, S. Airieau, and M. H. Thiemens (2001), Observation of wavelength-sensitive mass-independent sulfur isotope effects during SO₂ photolysis: Implications for the early atmosphere, *J. Geophys. Res.*, *106*, 32,829–32,840, doi:10.1029/2000JE001437.

Freeman, D. E., K. Yoshino, J. R. Esmond, and W. H. Parkinson (1984), High resolution absorption cross section measurements of SO₂ at 213 K in the wavelength region 172–240 nm, *Planet. Space Sci.*, *32*, 1125–1134, doi:10.1016/0032-0633(84)90139-9.

Hashimoto, G. L., and Y. Abe (2005), Climate control on Venus: Comparison of the carbonate and pyrite models, *Planet. Space Sci.*, *53*, 839–848, doi:10.1016/j.pss.2005.01.005.

Hearn, C. H., and J. A. Joens (1991), The near U.V. absorption spectrum of CS₂ and SO₂ at 300 K, *J. Quant. Spectrosc. Radiat. Transfer*, *45*, 69–75, doi:10.1016/0022-4073(91)90101-U.

Hegazi, E., F. Al-Adel, A. Dastageer, and A. Hamdan (1998), Zero-order ¹B₁(n,0,0) vibrational levels of sulfur dioxide, *J. Chem. Phys.*, *109*, 3928–3934, doi:10.1063/1.476992.

Hendrix, A. R., C. A. Barth, and C. W. Hord (1999), Io's patchy SO₂ atmosphere as measured by the Galileo ultraviolet spectrometer, *J. Geophys. Res.*, *104*, 11,817–11,826, doi:10.1029/1999JE900009.

Hermans, C., A. C. Vandaele, and S. Fally (2009), Fourier transform measurements of SO₂ absorption cross sections: I. Temperature dependence

in the 24 000–29 000 cm^{-1} (345–420 nm) region, *J. Quant. Spectrosc. Radiat. Transfer*, *110*, 756–765, doi:10.1016/j.jqsrt.2009.01.031.

Herzberg, G. (1966), *Molecular Spectra and Molecular Structure*, vol. 3, *Electronic Spectra and Electronic Structure of Polyatomic Molecules*, Krieger, Malabar, Fla.

Jessup, K. L., J. R. Spencer, G. E. Ballester, R. R. Howell, F. Roesler, M. Vigel, and R. Yelle (2004), The atmospheric signature of Io's Prometheus plume and anti-jovian hemisphere: Evidence for a sublimation atmosphere, *Icarus*, *169*, 197–215, doi:10.1016/j.icarus.2003.11.015.

Katagiri, H., T. Sako, A. Hishikawa, T. Yazaki, K. Onda, K. Yamanouchi, and K. Yoshino (1997), Experimental and theoretical exploration of photodissociation of SO₂ via the $\tilde{C}_1B_2$ state: Identification of the dissociation pathway, *J. Mol. Struct.*, *413*, 589–614, doi:10.1016/S0022-2860(97)00199-3.

Koplow, J. P., D. A. V. Kliner, and L. Goldberg (1998), Development of a narrow-band, tunable, frequency-quadrupled diode laser for UV absorption spectroscopy, *Appl. Opt.*, *37*, 3954–3960, doi:10.1364/AO.37.003954.

Krotkov, N. A., et al. (2008), Validation of SO₂ retrievals from the Ozone Monitoring Instrument over NE China, *J. Geophys. Res.*, *113*, D16S40, doi:10.1029/2007JD008818.

Kullmer, R. (1985), Vibronic coupling in SO₂, and its influence on the rotational structure of the bands in the 300–330 nm region, *Chem. Phys.*, *92*, 423–433, doi:10.1016/0301-0104(85)85036-9.

Lellouch, E. (2005), Io's atmosphere and surface-atmosphere interactions, *Space Sci. Rev.*, *116*, 211–224, doi:10.1007/s11214-005-1957-z.

Lyons, J. R. (2007), Mass-independent fractionation of sulfur isotopes by isotope-selective photodissociation of SO₂, *Geophys. Res. Lett.*, *34*, L22811, doi:10.1029/2007GL031031.

Manatt, S. L., and A. L. Lane (1993), A compilation of the absorption cross-sections of SO₂ from 106 to 403 nm, *J. Quant. Spectrosc. Radiat. Transfer*, *50*, 267–276, doi:10.1016/0022-4073(93)90077-U.

Martinez, R. D., and J. A. Joens (1992), SO₂ absorption cross-section measurements from 197 nm to 240 nm, *Geophys. Res. Lett.*, *19*, 277–279, doi:10.1029/91GL03165.

Marx, B. R., K. P. Birch, R. C. Felton, B. W. Jolliffe, W. R. C. Rowley, and P. T. Woods (1980), High-resolution spectroscopy of SO₂ using a frequency-doubled, continuous-wave dye laser, *Opt. Commun.*, *33*, 287–291, doi:10.1016/0030-4018(80)90245-X.

McGee, T. J., and J. Burris Jr. (1987), SO₂ absorption cross sections in the near U.V., *J. Quant. Spectrosc. Radiat. Transfer*, *37*, 165–182, doi:10.1016/0022-4073(87)90020-3.

Mills, F. P., and M. Allen (2007), A review of selected issues concerning the chemistry in Venus' middle atmosphere, *Planet. Space Sci.*, *55*, 1729–1740, doi:10.1016/j.pss.2007.01.012.

Murray, J. (1992), High resolution spectrometry of neutral chromium using a Fourier transform spectrometer, Ph.D. thesis, Imperial Coll. London, London.

Na, C. Y., L. W. Esposito, and T. E. Skinner (1990), International Ultraviolet Explorer observations of Venus SO₂ and SO, *J. Geophys. Res.*, *95*, 7485–7491, doi:10.1029/JD095iD06p07485.

Na, C. Y., L. W. Esposito, W. E. McClintock, and C. A. Barth (1994), Sulfur dioxide in the atmosphere of Venus. 2: Modeling results, *Icarus*, *112*, 389–395, doi:10.1006/icar.1994.1193.

Nave, G., R. C. M. Learner, A. P. Thorne, and C. J. Harris (1991), Precision Fe I and Fe II wavelengths in the ultraviolet spectrum of the iron-neon hollow-cathode lamp, *J. Opt. Soc. Am. B Opt. Phys.*, *8*, 2028–2041.

Okazaki, A., T. Ebata, and N. Mikami (1997), Degenerate four-wave mixing and photofragment yield spectroscopic study of jet-cooled SO₂ in the $\tilde{C}^1B_2$ state: Internal conversion followed by dissociation in the $\tilde{X}$ state, *J. Chem. Phys.*, *107*, 8752–8758, doi:10.1063/1.475168.

Pebler, A., and J. M. Zomp (1981), Stabilizing the radiant flux of a xenon arc lamp, *Appl. Opt.*, *20*, 4059–4061.

Pollack, J. B., O. B. Toon, R. C. Whitten, R. Boese, B. Ragent, M. Tomasko, L. Eposito, L. Travis, and D. Wiedman (1980), Distribution and source of the UV absorption in Venus' atmosphere, *J. Geophys. Res.*, *85*, 8141–8150, doi:10.1029/JA085iA13p08141.

Prahlad, V., S. M. Ahmed, and V. Kumar (1996), Temperature dependence of photoabsorption cross sections of sulphur dioxide at 280–320 nm, *J. Quant. Spectrosc. Radiat. Transfer*, *56*, 57–66, doi:10.1016/0022-4073(96)00021-0.

Rufus, J., G. Stark, P. L. Smith, J. C. Pickering, and A. P. Thorne (2003), High-resolution photoabsorption cross-section measurements of SO₂: 2. 220 to 325 nm at 295 K, *J. Geophys. Res.*, *108*(E2), 5011, doi:10.1029/2002JE001931.

Rufus, J., G. Stark, A. P. Thorne, J. C. Pickering, R. J. Blackwell-Whitehead, D. Blackie, and P. L. Smith (2009), High-resolution photoabsorption cross-section measurements of SO₂ at 160 K between 199 and 220 nm, *J. Geophys. Res.*, *114*, E06003, doi:10.1029/2008JE003319.

Sako, T., A. Hishikawa, and K. Yamanouchi (1998), Vibrational propensity in the predissociation rate of SO₂($\tilde{C}^1B_2$) by two types of nodal patterns in vibrational wavefunctions, *Chem. Phys. Lett.*, *294*, 571–578, doi:10.1016/S0009-2614(98)00922-1.

Sartoretti, P., M. J. S. Belton, and M. A. McGrath (1996), SO₂ distributions on Io, *Icarus*, *122*, 273–287, doi:10.1006/icar.1996.0125.

Shaw, R. J., J. E. Kent, and M. F. O'Dwyer (1980), Single vibronic level fluorescence spectra of sulfur dioxide, *J. Mol. Spectrosc.*, *82*, 1–26, doi:10.1016/0022-2852(80)90096-X.

Speidel, M., R. Nau, F. Arnold, H. Schlager, and A. Stohl (2007), Sulfur dioxide measurements in the lower, middle and upper troposphere: Deployment of an aircraft-based chemical ionization mass spectrometer with permanent in-flight calibration, *Atmos. Environ.*, *41*(11), 2427–2437, doi:10.1016/j.atmosenv.2006.07.047.

Spencer, J. R., et al. (2007), Io volcanism seen by new horizons: A major eruption of the Tvashtar Volcano, *Science*, *318*, 240–243, doi:10.1126/science.1147621.

Stark, G., P. L. Smith, J. Rufus, A. P. Thorne, J. C. Pickering, and G. Cox (1999), High-resolution photoabsorption cross-section measurements of SO₂ at 295 K between 198 and 220 nm, *J. Geophys. Res.*, *104*, 16,585–16,590, doi:10.1029/1999JE001022.

Svedhem, H., et al. (2007), Venus Express—The first European mission to Venus, *Planet. Space Sci.*, *55*, 1636–1652, doi:10.1016/j.pss.2007.01.013.

Swedish Environmental Protection Agency (1990), *Air Pollution '90*, Norstedts Tryckeri, Stockholm.

Taylor, F., and D. Grinspoon (2009), Climate evolution of Venus, *J. Geophys. Res.*, *114*, E00B40, doi:10.1029/2008JE003316.

Thorne, A. P., C. J. Harris, I. Wynne-Jones, R. C. M. Learner, and G. Cox (1987), A Fourier transform spectrometer for the vacuum ultraviolet: Design and performance, *J. Phys. E: Sci. Instrum.*, *20*, 54–60, doi:10.1088/0022-3735/20/1/010.

Vandaele, A. C., P. C. Simon, J. M. Guilmot, M. Carleer, and R. Colin (1994), SO₂ absorption cross section measurement in the UV using a Fourier transform spectrometer, *J. Geophys. Res.*, *99*, 25,599–25,605, doi:10.1029/94JD02187.

Vattulainen, J., J. Stenberg, R. Hernberg, L. Wallenius, and V. Linna (1997), Experimental determination of SO₂, C₂H₂, and O₂ UV absorption cross sections at elevated temperatures and pressures, *Appl. Spectrosc.*, *51*, 1311–1315, doi:10.1366/0003702971942312.

Woods, P. T., B. W. Jolliffe, and B. R. Marx (1984), High-resolution spectroscopy of SO₂ using a frequency-doubled pulsed dye laser, with application to the remote sensing of atmospheric pollutants, *Opt. Commun.*, *33*, 281–286, doi:10.1016/0030-4018(80)90244-8.

Wu, C. Y. R., and D. L. Judge (1981), SO₂ and CS₂ cross section data in the ultraviolet region, *Geophys. Res. Lett.*, *8*, 769–771.

Wu, C. Y. R., T. S. Chien, G. S. Liu, D. L. Judge, and J. J. Caldwell (1989), Photoabsorption and direct dissociation cross sections of C₂H₂ in the 1530–1930 Å region—A temperature dependent study, *J. Chem. Phys.*, *91*, 272–280, doi:10.1063/1.457513.

Wu, C. Y. R., B. W. Yang, F. Z. Chen, D. L. Judge, J. Caldwell, and L. M. Trafton (2000), Measurements of high-, room-, and low-temperature photoabsorption cross sections of SO₂ in the 2080- to 2950-Å region, with application to Io, *Icarus*, *145*, 289–296, doi:10.1006/icar.1999.6322.

Yamanouchi, K. (1995), Laser induced fluorescence spectroscopy of the C¹B₂/X¹A₁ band of jet-cooled SO₂: Rotational and vibrational analyses in the 235–210 nm region, *J. Mol. Struct.*, *352*, 541–559, doi:10.1016/0022-2860(95)08835-J.

Zasova, L. V., N. Ignatiev, I. Khatuntsev, and V. Linkin (2007), Structure of the Venus atmosphere, *Planet. Space Sci.*, *55*, 1712–1728, doi:10.1016/j.pss.2007.01.011.

D. Blackie, J. C. Pickering, J. Rufus, and A. P. Thorne, Space and Atmospheric Physics Group, Imperial College London, Huxley Building, London SW7 2AZ, UK. (douglas.blackie01@imperial.ac.uk)

R. Blackwell-Whitehead, Lund Observatory, SE-221 00 Lund, Sweden.

P. L. Smith, Harvard-Smithsonian Center for Astrophysics, Cambridge, MA 02138, USA.

G. Stark, Department of Physics, Wellesley College, Wellesley, MA 02481, USA.